



Murdoch
UNIVERSITY

MURDOCH RESEARCH REPOSITORY

<http://researchrepository.murdoch.edu.au/14203/>

Hettiwatte, S.N., Kirton, R.S., Kuijer, J.P.A., Epstein, F.H., Cowan, B.R. and Young, A.A. (2007) Comparison of SPAMM, HARP and DENSE in a Deformable Phantom. In: Proceedings of the Society for Cardiovascular Magnetic Resonance 2007. Journal of Cardiovascular Magnetic Resonance, Vol. 9, No. 2, pp. 351-352.

It is posted here for your personal use. No further distribution is permitted.

504. DETECTION OF PERI-INFARCT ZONE BY DELAYED-ENHANCEMENT MAGNETIC RESONANCE AND MULTIDETECTOR COMPUTED TOMOGRAPHY IMAGING IN POST-MYOCARDIAL INFARCTION CARDIOMYOPATHY

Marco Centola, MD, Karl Heinz Schuleri, MD, Richard George, MD, Robert Evers, Kristina Evers, Andrea Vavere, Joshua Hare, MD, Albert C. Lardo, PhD. *Johns Hopkins University, Baltimore, MD, USA.*

Background: The extent of peri-infarct zone characterized by delayed-enhancement magnetic resonance (DE-MR) provides an incremental prognostic value besides the left ventricular systolic volume index and the ejection fraction in post-myocardial infarction cardiomyopathy. The recent advent of delayed contrast-enhanced multidetector computed tomography (MDCT) is expanding its potential for an accurate evaluation of myocardial necrosis, microvascular obstruction and collagenous chronic scar following the MI. However, the ability of MDCT to detect and quantify the peri-infarct zone is unknown. Accordingly, we hypothesized that MDCT can accurately identify the peri-infarct zone in occlusion/reperfusion animal model of chronic MI compared to DE-MRI.

Methods and Results: Eight Göttingen minipigs underwent 120 to 150 minute coronary artery occlusion followed by reperfusion. MDCT and MR studies were performed on the same day 6 months after MI induction followed by animal sacrifice. Delayed contrast-enhanced MDCT images were acquired on a 64-slice CT scanner (Toshiba) with an axial slice thickness of 0.5 mm five minutes after 150 mL iodine contrast injection. For infarct size analysis CT-images were reconstructed at 2 and 8 mm. Delayed enhancement MR was performed 15–20 minutes following 0.2 $\mu\text{m}/\text{kg}$ Gd-DTPA the same day using an inversion-recovery gradient-echo pulse sequence and slice thickness of 8 mm on a 1.5 T scanner (GE). Semi-automated quantitative analyses were performed using a uniform threshold technique of the remote myocardium to the infarct areas. The peri-infarct zone was normalized as a percentage of the infarct size. Mean DE-MR-defined infarct size at 6 months post-MI was $19.6 \pm 2.1\%$ of left ventricular (LV) volume. The infarct size characterized by MDCT at 8 mm slice thickness correlated well with MR ($r = 0.659$; $p < 0.05$). The peri-infarct size detected by MRI showed a good correlation with MDCT at 8 mm ($0.9 \pm 0.4\%$ versus 1.1 ± 0.2 , mean difference 0.2%). Interestingly, subsequent analysis in 4 animals could demonstrate that the peri-infarct size characterized by MDCT at 2 mm ($0.2 \pm 0.06\%$) did not match well with that measured by MR and MDCT 8 mm.

Conclusion: The spatial extent of chronic myocardial infarction and peri-infarct zone can be determined and quantified accurately with delayed contrast enhanced-MDCT compared to MR. However, the reduction of slice thickness by MDCT can better characterize the peri-infarct zone because of the decrease

in partial volume effects. Further studies will elucidate the ideal slice thickness of delayed enhancement MDCT imaging for accurate peri-infarct zone measurements.

505. COMPARISON OF SPAMM, HARP AND DENSE IN A DEFORMABLE PHANTOM

Sujeewa N. Hettiwatte, PhD,¹ Robert S. Kirton, PhD,¹ Joost P. A. Kuijper, PhD,² Frederick H. Epstein, PhD,³ Brett R. Cowan, MBChB,⁴ Alistair A. Young, PhD.⁵
¹Bioengineering Institute, University of Auckland, Auckland, New Zealand, ²Vrije Universiteit Medical Center, Amsterdam, The Netherlands, ³Departments of Radiology and Biomedical Engineering, University of Virginia, Charlottesville, VA, USA, ⁴Centre for Advanced MRI, Faculty of Medical and Health Sciences, University of Auckland, Auckland, New Zealand, ⁵Department of Anatomy with Radiology and Bioengineering Institute, University of Auckland, Auckland, New Zealand.

Introduction: A number of techniques are available for the measurement of displacement and strain in the heart including SPATial Modulation of Magnetization (SPAMM) (1) followed by tag line detection, CSPAMM followed by Harmonic Phase (HARP) analysis (2), and Displacement Encoding with Stimulated Echoes (DENSE) (3). However, it is unclear which method gives the most accurate results in practice.

Purpose: This study compared SPAMM, HARP and DENSE imaging of a deformable gel phantom by comparing the accuracy of pixel-based displacement and strain measurements from each technique with a known analytical solution.

Methods: A deformable, silicone gel cylindrical annulus with a fixed outer cylinder (radius 50 mm) and movable inner cylinder (radius 20 mm) was cyclically driven at 1Hz by a stepper motor to rotate the inner cylinder by 45 deg in a sinusoidal fashion. The deformation has an analytical solution independent of material properties of the gel (4). Images were obtained on a 1.5T Siemens Avanto.

TrueFISP SPAMM tagging (1) used FOV 300×300 mm, grid tagging 45 deg to readout direction with 7 mm spacing, image matrix 256×154 interpolated to 256×256 , slice thickness 8 mm, TR 18.64 ms, TE 2.33 ms, flip 20 deg, 8 segments, bandwidth 370 Hz/pixel, tag flip 122 deg, 5 LISA cycles, 49 frames, single ~ 20 s acquisition. TrueFISP 1-1 CSPAMM HARP (2) used FOV 300×300 mm, line tagging in the readout direction at 7 mm spacing, image matrix 256×77 interpolated to 256×256 , slice thickness 8 mm, TR 18.64 ms, TE 2.33 ms, flip 20 deg, 8 segments, bandwidth 370 Hz/pixel, tag flip 140 deg, 5 LISA cycles, 49 frames, single ~ 20 s acquisition (two encoding directions). CineDENSE imaging (3) used FOV 300×225 mm, 1-1 CSPAMM at $k_{\text{enc}} = 0.2$ cycles/mm, image matrix 128×96 ,

TABLE
Errors (mean \pm sd) in displacements and Eulerian strains

	Angular displacement (Uth, degrees)	Radial displacement (Ur, mm)	Radial strain (Err)	Circumferential strain (Ecc)	Shear strain (Erc)
SPAMM	-3.80 ± 1.28	-0.72 ± 0.60	-0.05 ± 0.09	-0.02 ± 0.03	0.07 ± 0.06
HARP	-0.34 ± 0.27	0.02 ± 0.14	-0.01 ± 0.04	0.00 ± 0.01	0.01 ± 0.03
DENSE	-0.29 ± 0.70	-0.12 ± 0.39	-0.01 ± 0.05	0.00 ± 0.03	0.01 ± 0.03

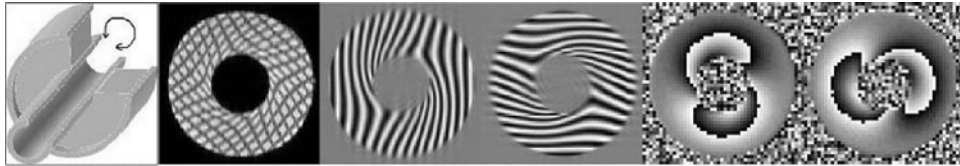


FIG. 1. Left to right: Cut-away view of phantom, deformed SPAMM grid-tagged image, x and y complementary-SPAMM images used in HARP, and x and y phase images used in DENSE.

slice thickness 8 mm, TR 20 ms, TE 5.75 ms, flip 15 deg, 14 segments, EPI factor 7, bandwidth 798 Hz/pixel, tag flip 180 deg, 23 frames, two ~ 20 s acquisitions (one for each encoding direction).

In SPAMM, the grid-tagged images were convolved with the 2nd derivative of a Gaussian to obtain tag lines in each direction. The distance from each pixel to the closest tag minimum was obtained by searching along a straight line normal to the initial undeformed tags. Displacement maps were then calculated as the difference from the first frame. Such displacements are accurate only at tag line centers; at all other points, the displacements were calculated using a thin-plate spline interpolation. In HARP, the phase of the filtered image provided position information at each pixel and displacements were calculated from the phase differences from the first frame. The k-space filter was circular, centered at the harmonic peak at $d = 1/7$ cycles/mm, with radius

0.8 d, and Gaussian roll off. In DENSE, the image phase gave the displacements directly at each pixel (no filters were applied). With all three methods phase unwrapping was required to obtain the actual displacements in two orthogonal directions, which were then used to calculate Eulerian strain using a pixel based algorithm.

Results: The mean and standard deviation of errors between phantom results and the analytic solution were calculated at every pixel within a mask of $R = 25$ mm to 45 mm (Table). Fig. 1 shows a cut-away view of the phantom, and images obtained by each technique, and Fig. 2 shows the variation in radial Eulerian strain (Err) averaged at each radius.

Conclusions: Phantom experiments showed that errors in displacements and strains were small in DENSE and HARP, and highest in SPAMM. Errors in SPAMM were likely due to the very simple pixel based tag tracking algorithm used.

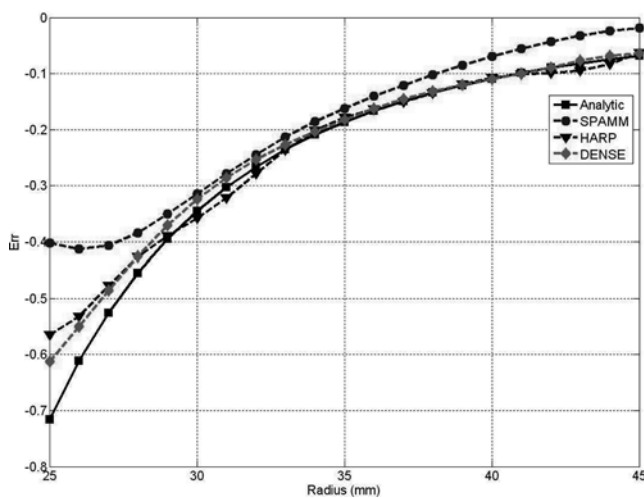


FIG. 2. Variation of Eulerian radial strain (Err) with radius.

REFERENCES

1. Zwanenburg et al. MRM 2003; 49:722–730.
2. Kuijter et al. MRM 2001; 46:993–999.
3. Kim et al. Radiology 2004; 230:862–871.
4. Young et al. Radiology 1993; 188:101–108.

506. WALL THICKNESS IN HUMAN CAROTID ARTERIES CORRELATES NEGATIVELY WITH PLAQUE INFLAMMATION AS DETERMINED BY FDG PET

James H. F. Rudd, MD, PhD, Karen Weinshelbaum, Venkatesh Mani, PhD, Kelly Myers, Sameer Bansilal, MD, Michael Farkouh, MD, Josef Machac, MD, Silvia Aguiar, MD, Valentin Fuster, MD, PhD, Zahi A. Fayad, PhD. *Mount Sinai School of Medicine, New York, NY, USA.*